

10176

ОБЪЕДИНЕННЫЙ
ИНСТИТУТ
ЯДЕРНЫХ
ИССЛЕДОВАНИЙ

ДУБНА



10176

E2 - 10176

Экз. чит. зала

S.T.Petrov

THE NEUTRINO MIXING

AND THE $\mu \rightarrow e + \gamma$, $\mu \rightarrow e + e + \bar{e}$

AND $\nu' \rightarrow \nu + \gamma$ DECAYS

1976

E2 - 10176

S.T.Petcov

THE NEUTRINO MIXING

AND THE $\mu \rightarrow e + \gamma$, $\mu \rightarrow e + e + \bar{e}$

AND $\nu' \rightarrow \nu + \gamma$ DECAYS

Submitted to ЯФ



I. Neutrino mixing and neutrino oscillations are widely discussed in the physical literature ^{/1-6/}. One possible way ^{/4,6/} to introduce the neutrino mixing in the theory of weak interaction of the four observed leptons is to construct the weak leptonic charged current in full analogy with the weak charged current of the four quarks of the GIM model ^{/7/} :

$$j_a^\theta = \bar{\mu} \gamma_a (1 + \gamma_5) \nu_\mu^\theta + \bar{e} \gamma_a (1 + \gamma_5) \nu_e^\theta, \quad (1)$$

where

$$\begin{aligned} \nu_\mu^\theta &= -\nu \sin \theta + \nu' \cos \theta, \\ \nu_e^\theta &= \nu \cos \theta + \nu' \sin \theta, \end{aligned} \quad (2)$$

ν and ν' are massive neutrino fields (with masses m and m' , respectively) and θ is a parameter analogous to the Cabibbo angle.

The Lagrangian of the modified Weinberg-Salam model ^{/8/} with the charged leptonic current of the form (1) does not contain

nonsymmetric neutral currents. The latter appear effectively in the higher orders admitting the processes

$$\mu \rightarrow e + \gamma, \quad (3)$$

$$\mu \rightarrow e + e + \bar{e}, \quad (4)$$

$$\nu' \rightarrow \nu + \gamma \quad (5)$$

Note that the decays (3)-(5) are analogous to the hadronic $\Delta S \neq 0$, $\Delta Q = 0$ decays in the GIM model (for example, $K \rightarrow \pi \nu \bar{\nu}$).

A theory with the charged leptonic current (1) predicts also the existence of neutrino oscillations. The latter were considered in detail in ref./4/.

In this note we shall evaluate the decay rates of the processes (3)-(5) in the modified according to (1) and (2) Weinberg-Salam model. In the following calculations we shall neglect terms smaller than $(\frac{m_\ell^2}{M_w^2})^2$ ($\ell = \mu, e, \nu, \nu', M_w$

is the mass of the charged vector boson of the Weinberg-Salam model, $M_w \geq 37,3$ GeV, $M_w \gg m_\ell$). The decays $\mu \rightarrow e + \gamma$ and $\nu' \rightarrow \nu + \gamma$ were also considered in ref./6/ but the corresponding amplitudes used to calculate the decay rates of these processes are not gauge invariant since some of the diagrams contributing to these amplitudes are not accounted. For example, in the case of $\mu \rightarrow e + \gamma$ decay the authors of ref./6/ considered the contribution only of six diagrams instead of the sixteen needed (in the 't Hooft-Feynman gauge). Our calculations lead to gauge invariant amplitudes and our results considerably differ from the results obtained in ref./6/

II. The masses of the two neutrinos ν' and ν must be introduced in the Weinberg-Salam model without destroying its renormalizability by means of the mechanism of spontaneous symmetry breaking /9/ (the Higgs mechanism). This can be achieved by adding to the initial Weinberg-Salam Lagrangian with zero mass fields the gauge invariant terms:

$$\Delta \mathcal{L} = - \frac{m}{M_w} g \{ (\bar{L}_e \phi^c \cos \theta - \bar{L}_\mu \phi^c \sin \theta) \nu_R + \text{h.c.} \} - \quad (6)$$

$$- \frac{m'}{M_w} g \{ (\bar{L}_e \phi^c \sin \theta + \bar{L}_\mu \phi^c \cos \theta) \nu'_R + \text{h.c.} \}.$$

Here

$$\nu_R = \frac{1}{2} (1 - \gamma_5) \nu, \quad \nu'_R = \frac{1}{2} (1 - \gamma_5) \nu',$$

$$\frac{g^2}{8M_w^2} = \frac{G_F}{\sqrt{2}}, \quad L_{e(\mu)} = \begin{pmatrix} \nu_{e(\mu)}^\theta \\ e(\mu) \end{pmatrix},$$

$\phi^c \equiv i\tau_2 \phi^*$, ϕ is the scalar doublet of the Weinberg-Salam model. The terms (6) generate the mass terms of the fields ν and ν' via spontaneous symmetry breaking.

Let us consider now the decays (3)-(5). All the necessary calculations will be done in the 't Hooft-Feynman gauge. The evaluation of the amplitudes of the decays $\mu \rightarrow e + \gamma$ and $\mu \rightarrow e + e + \bar{e}$ is given in the Appendix. The relevant part of the interaction Lagrangian has the following form in the 't Hooft-Feynman gauge:

$$\mathcal{L} = i \frac{g}{2\sqrt{2}} (W_a^- j_a + \text{h.c.}) + i \frac{(g^2 + g'^2)^{1/2}}{4} Z_a j_a^z +$$

$$\begin{aligned}
& + ieA_a j_a^{em} + i(eA_{\beta^+} g \cos \theta_w Z_{\beta}) \{W_a^- (\partial_a W_{\beta^+}^+ \\
& - \partial_{\beta} W_a^+) + W_a^+ (\partial_{\beta} W_a^- - \partial_a W_{\beta}^-) + \partial_a (W_a^- W_{\beta^+}^+ \\
& - W_{\beta}^- W_a^+) \} + (eA_a - \frac{1}{2}(g^2 + g'^2)^{1/2} \cos 2\theta_w Z_a) \{M_w (W_a^- s^+ + \\
& + h.c.) + i(s^- \partial_a s^+ - \partial_a s^- s^+) \} - \{ \frac{m_e}{M_w} g (L_e \phi e_R + \\
& + h.c.) + (e \rightarrow \mu) \} + \Delta \mathcal{L}.
\end{aligned}$$

Here Z_a and M_z are the field and mass of the neutral vector boson, θ_w is the Weinberg angle, s^{\pm} and ψ are the Goldstone bosons, χ is the Higgs scalar, $\sqrt{2}(g^2 + g'^2) = 8M_Z^2 G_F$

$$g \tan \theta_w = g', \quad e_R = \frac{1}{2}(1 - \gamma_5)e, \quad \mu_R = \frac{1}{2}(1 - \gamma_5)\mu,$$

$$\phi = \frac{1}{\sqrt{2}} \begin{pmatrix} s^+ \\ \chi + i\psi \end{pmatrix}, \quad j_a^{em} = \bar{\mu} \gamma_a \mu + \bar{e} \gamma_a e,$$

$$j_a^Z = (\nu \gamma_a (1 + \gamma_5) \nu + (\nu \rightarrow \nu')) - (e \gamma_a (1 + \gamma_5 - 4 \sin^2 \theta) e + (e \rightarrow \mu)).$$

The diagrams contributing to the process $\mu \rightarrow e + \gamma$ are shown in Fig.1. The evaluation of these diagrams leads to the gauge-invariant amplitude (see the Appendix):

$$M_1 = \frac{G_F e}{8\pi^2 \sqrt{2}} \frac{m'^2 - m^2}{M_w^2} \sin \theta \cos \theta \frac{1}{4} \bar{u}(p') (1 - \gamma_5) \times \quad (7)$$

$$\times m_{\mu} \sigma_{\rho\alpha} q_{\alpha} u(p) \xi_{\rho}(q),$$

where p' and p are the electron and muon momenta, $q = p - p'$ and $\xi_{\rho}(q)$ is the photon polarization vector. Notice that there is a deep mutual compensation of the contributions of diagrams which differ only by the virtual neutrino. This compensation mechanism is analogous to the GIM mechanism of compensation of the diagrams of the hadronic weak $\Delta S \neq 0, \Delta Q = 0$ processes^{/10/}.

For the $\mu \rightarrow e + \gamma$ decay rate we have:

$$\Gamma(\mu \rightarrow e + \gamma) = \frac{1}{16} \frac{G_F^2 m^5}{128 \pi^3} \frac{\alpha}{\pi} \frac{(m'^2 - m^2)^2}{M_w^2} \sin^2 \theta \cos^2 \theta. \quad (8)$$

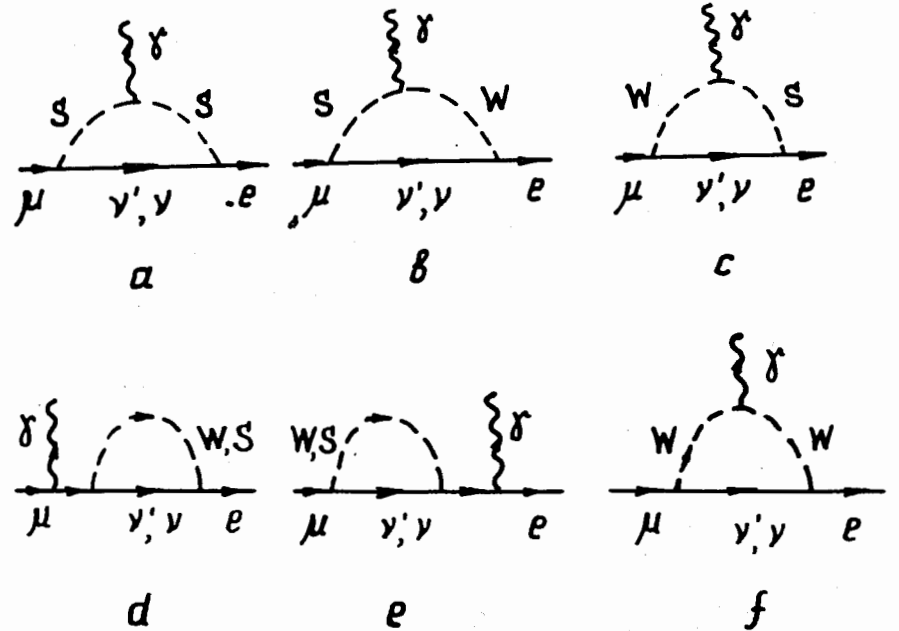


Fig. 1. Third order diagrams for $\mu \rightarrow e + \gamma$.

Our expression for $\Gamma(\mu \rightarrow e + \gamma)$ differs from that obtained in ref./6/ by the multiplicative factor of $5 \cdot 10^{-4} (m_\mu / M_w)^4$.

Let us compare the expression (8) for the $\Gamma(\mu \rightarrow e + \gamma)$ with the existing experimental data. The value of $\Gamma(\mu \rightarrow e + \gamma)$ depends on three parameters m', m and θ . If the angle θ is regarded as a free parameter and if $m' \gg m$ then the existing data lead to the restrictions/6/:

$$\begin{aligned} \sin^2 \theta &\leq 10^{-2} \\ m' &< 0.9 \text{ MeV} \\ m &< 35 \text{ eV} \end{aligned} \quad (A)$$

In ref./4/ it was suggested that $\theta = \frac{\pi}{4}$ (maximal mixing) and the analysis of the experimental data in this case leads to

$$\begin{aligned} |m' - m| &\leq 10^{-1} \text{ eV} \\ m', m &< 35 \text{ eV} \end{aligned} \quad (B)$$

All subsequent numerical estimates will be derived in these two extreme cases.

So, for the ratio of the $\mu \rightarrow e + \gamma$ decay rate to the $\mu \rightarrow e + \nu_\mu + \bar{\nu}_e$ decay rate we have:

$$\Gamma(\mu \rightarrow e + \gamma) / \Gamma_\mu < \begin{cases} 6,2 \cdot 10^{-25} & \text{case (A)} \\ 2,4 \cdot 10^{-45} & \text{case (B)}, \end{cases}$$

which is at least by seventeen orders smaller than the experimental upper bound:

$$(\Gamma(\mu \rightarrow e + \gamma) / \Gamma_\mu)_{\text{exp}} < 2,2 \cdot 10^{-8} / 11/$$

III. We turn now to the process $\mu \rightarrow e + e + \bar{e}$. The diagrams of Fig.1 with virtual photon converting into $e^+ e^-$ pair and the diagrams of Fig.2 contribute to this decay.

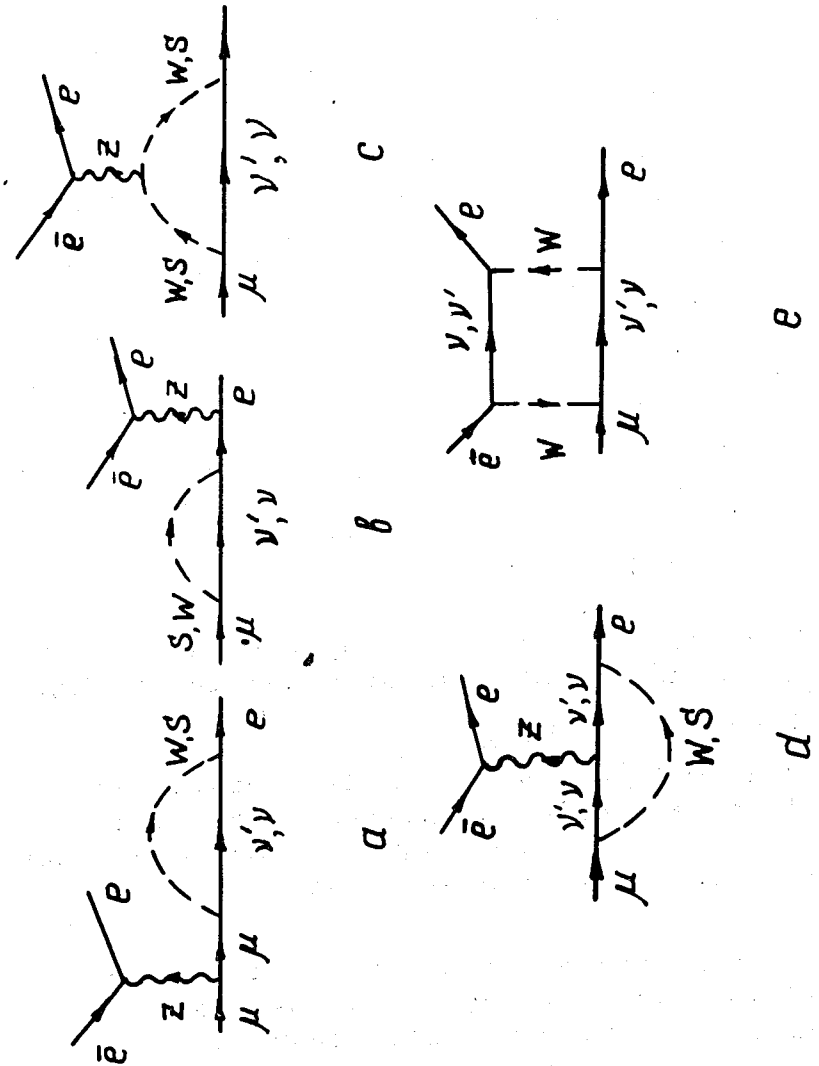


Fig. 2. Important fourth order diagrams for $\mu \rightarrow e + e + \bar{e}$.

Obviously, the relevant amplitude must be antisymmetrized with respect to the states of the two electrons. The calculations give the following expression for the amplitude of the $\mu \rightarrow e+e+\bar{e}$ process (see the Appendix):

$$M_2 = i \frac{G_F a}{2\pi\sqrt{2}} \frac{m'^2 - m^2}{M_w^2} \ln \frac{M_w^2}{m'^2} \sin\theta \cos\theta \times \quad (9)$$

$$\times \bar{u}(k_1)\gamma_\rho(1+\gamma_5)u(p)\bar{u}(k_2)\gamma_\rho(1-(1+\gamma_5)/(8\sin^2\theta_w))u(-k_3)-(k_1 \leftrightarrow k_2).$$

It is easy now to evaluate the $\mu \rightarrow e+e+\bar{e}$ decay rate:

$$\Gamma(\mu \rightarrow e+e+\bar{e}) = \frac{G_F^2 m_\mu^5}{128\pi^3} \frac{a^2}{4\pi^2} \left(\frac{m'^2 - m^2}{M_w^2} \ln \frac{M_w^2}{m'^2} \right)^2 \sin^2\theta \cos^2\theta \times$$

$$\times \left(\frac{1}{3} + (1 - 1/(4\sin^2\theta_w))^2 \right).$$

So, with $\sin^2\theta_w = 0,3$ we get for the ratio $\Gamma(\mu \rightarrow e+e+\bar{e})/\Gamma_\mu$:

$$\Gamma(\mu \rightarrow e+e+\bar{e})/\Gamma_\mu < \begin{cases} 8 \cdot 10^{-25} & \text{case (A)} \\ 10^{-44} & \text{case (B)}. \end{cases}$$

The best experimental upper bound for the $\mu \rightarrow e+e+\bar{e}$ decay rate was obtained in ref./12/:

$$(\Gamma(\mu \rightarrow e+e+\bar{e})/\Gamma_\mu)_{\text{exp}} < 1.9 \cdot 10^{-9}$$

Thus we see that the model considered predicts essentially smaller upper bounds for the $\mu \rightarrow e+\gamma$ and $\mu \rightarrow e+e+\bar{e}$ decay rates than the existing experimental ones.

IV. The masses of the two neutrinos of the model are not equal. Suppose that $m' > m$. Then the neutrino ν' will decay into the neutrino ν with emission of a photon. The diagrams for this process are shown in Fig.3.

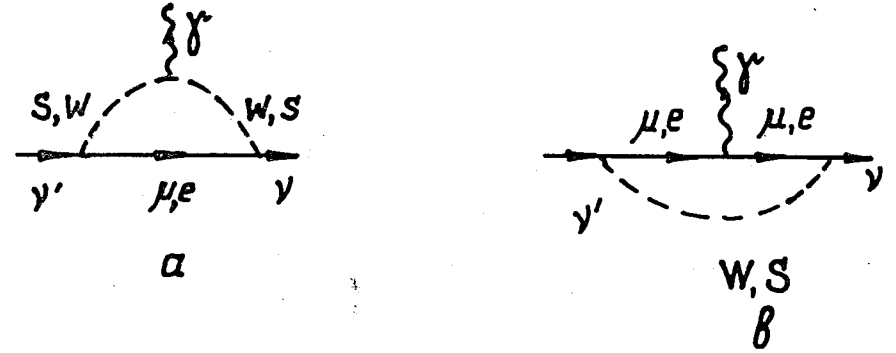


Fig. 3. Diagrams contributing to the $\nu' \rightarrow \nu + \gamma$ decay amplitude.

The leading contribution to the $\nu' \rightarrow \nu + \gamma$ amplitude comes from the gauge invariant part of the diagrams of fig.3b with the virtual W-boson:

$$M_3 = \frac{G_F e}{8\pi^2\sqrt{2}} \frac{m_\mu^2}{M_w^2} \ln \frac{M_w^2}{m_\mu^2} \sin\theta \cos\theta \bar{u}(p')(m+m') \times \quad (10)$$

$$\times \sigma_{\rho\alpha} q_\alpha (1 - \gamma_5 \frac{m' - m}{m' + m}) u(p) \bar{\xi}_\rho(q).$$

The $\nu' \rightarrow \nu + \gamma$ decay rate is of the form:

$$\Gamma(\nu' \rightarrow \nu + \gamma) = \frac{G_F^2 m'^5}{128\pi^3} a \sin^2\theta \cos^2\theta \left(1 - \frac{m^2}{m'^2}\right)^3 \left(1 + \frac{m^2}{m'^2}\right) \times$$

$$\times \left(\frac{m_\mu^2}{M_w^2} \ln \frac{M_w^2}{m_\mu^2} \right)^2$$

and its value in both cases (A) and (B) is too small to affect the Solar neutrino oscillations predicted by the model.

APPENDIX

The $\mu \rightarrow e + \gamma$, $\mu \rightarrow e + e + \bar{e}$ and $\nu' \rightarrow \nu + \gamma$ amplitudes

We shall treat the divergent diagrams by means of the dimensional regularization^{/14/} procedure which preserves gauge invariance. Formally, the dimensional regularization implies generalization of the dimension of the momentum space from 4 to n , where n is, in general, a complex parameter. The regularization is switched off by the limiting procedure $n \rightarrow 4$ after the momentum integration is performed. In the theory of the dimensional regularization the divergent integrals lead to terms which have poles at $n = 4$.

Let us consider now the effective ($\mu e \gamma$) vertex $\Gamma_\rho(q)$ (q is the momentum of the photon) which in the lowest order is generated by the diagrams shown in Fig.1. When evaluating the $\mu \rightarrow e + e + \bar{e}$ amplitude we shall need the form of the vertex for $q^2 \neq 0$ so we shall assume that the photon is not on the mass shell. The diagrams of Fig. 1a-c and Fig. 1f have both gauge invariant and gauge noninvariant parts while the diagrams of Fig. 1d-c have no gauge invariant parts. Let us write down the contribution of the gauge noninvariant part of each diagram of Fig. 1 up to the terms of order $eg^2 \frac{m'^2 - m^2}{M_w^2}$ as coefficients multiplying the factor

$$e \frac{G_F}{\sqrt{2}} \sin\theta \cos\theta \frac{m'^2 - m^2}{16\pi^2} \gamma_\rho (1 + \gamma_5),$$

V. Let us summarize briefly the main results of the present note. We have evaluated the $\mu \rightarrow e + \gamma$, $\mu \rightarrow e + e + \bar{e}$ and $\nu' \rightarrow \nu + \gamma$ decay rates in the modified Weinberg-Salam model with neutrino mixing. For the values of the parameters of the theory (m', m and θ) allowed by the experimental data the $\mu \rightarrow e + \gamma$ and $\mu \rightarrow e + e + \bar{e}$ decay rates are essentially smaller than the corresponding experimental upper bounds. Thus we come to the conclusion that our results indicate the actuality of the Solar neutrino oscillation experiments proposed by B.Pontecorvo^{/13/}. They measure amplitudes instead of amplitudes squared in such experiments. So, these experiments are highly sensitive for verifying the considered scheme of neutrino mixing. The calculations performed show that the instability of the heavier neutrino does not affect the neutrino oscillations.

The author expresses his deep gratitude to Dr. S.M.Bilenky for suggesting the problem and his regular interest in the course of the work. The author is also grateful to Dr. A.A.Slavnov for usefull discussions on renormalization of the gauge theories.

$$\Gamma(1a) = -\left(\frac{1}{2} + \frac{2}{4-n} + C\right), \quad \Gamma(1b+1c) = -4,$$

$$\Gamma(1d) = 2\left(1 + \frac{2}{4-n} + C\right) + \left(\frac{1}{2} + \frac{2}{4-n} + C\right) - 2,$$

$$\Gamma(1e) = -2\left(1 + \frac{2}{4-n} + C\right), \quad \Gamma(1f) = 6,$$

where C is a constant. The sum of these terms is equal to zero. Let us note that the cancellation of the gauge noninvariant contributions to $\Gamma_\rho(q)$ does not depend on the approximation used to derive them. The evaluation of the gauge invariant contributions of the diagrams of Fig. 1 leads to the following expression for the $\Gamma_\rho(q)$:

$$\begin{aligned} \Gamma_\rho(q) = & e \frac{G_F}{8\pi^2\sqrt{2}} \sin\theta \cos\theta \frac{m'^2 - m^2}{M_w^2} \left\{ \left(\frac{1}{4} - \frac{5}{12} + \frac{5}{12}\right) \times \right. \\ & \times (m_\mu + m_e) \sigma_{\rho\alpha} q_\alpha (1 - \gamma_5) \frac{m_\mu - m_e}{m_\mu + m_e} + \left(\frac{1}{2} + \frac{4}{9} + \frac{1}{18}\right) \times \\ & \left. \times (\gamma_\rho q^2 - \gamma_\alpha q_\alpha q_\rho) (1 + \gamma_5) \right\}, \end{aligned} \quad (A.1)$$

where the sum of the term with factor $\frac{1}{4}$ and that with factor $\frac{1}{2}$ is due to the contribution of Fig. 1a, the sum of the term with factor $(-\frac{5}{12})$ and that with factor $\frac{1}{18}$ is due to the contribution of Fig. 1b and Fig. 1c, and the sum of the term with factor $\frac{5}{12}$ and that with factor $\frac{4}{9}$, respectively, to Fig. 1f. Knowing that for the on-shell photon $q^2 = 0$, $q_\rho \xi_\rho(q) = 0$ ($\xi_\rho(q)$ is the photon polarization vector) it is easy to find now the $\mu \rightarrow e + \gamma$ amplitude:

$$\begin{aligned} M_1 = & \frac{G_F e}{8\pi^2\sqrt{2}} \frac{m'^2 - m^2}{M_w^2} \sin\theta \cos\theta \bar{u}(p') \frac{1}{4} (1 - \gamma_5) m_\mu \times \\ & \times \sigma_{\rho\alpha} q_\alpha u(p) \xi_\rho(q), \end{aligned} \quad (A.2)$$

where p and p' are the momenta of the muon and the electron, respectively.

In the one-loop approximation we work the $\mu \rightarrow e + e + \bar{e}$ amplitude may be expressed as a sum of three terms

$$M_2 = M^{(\gamma)} + M^{(w)} + M^{(z)}, \quad (A.3)$$

where the $M^{(\gamma)}$ term corresponds to the contribution of the diagrams shown in Fig. 1 with virtual photon converting into e^+e^- pair, $M^{(w)}$ - to the contribution of the diagrams of Fig. 2e, and $M^{(z)}$ - to the contribution of diagrams of Fig. 2 with virtual Z -boson. The evaluated $\mu e \gamma$ vertex determines $M^{(\gamma)}$:

$$M^{(\gamma)} = ie \bar{u}(k_1) \Gamma_\rho(p - k_1) u(p) \frac{1}{(p - k_1)^2} \bar{u}(k_2) \gamma_\rho u(-k_3) - (k_1 \leftrightarrow k_2), \quad (A.4)$$

where k_1 , k_2 and k_3 are the momenta of the two electrons and the positron, respectively.

The terms proportional to the masses and momenta of the real particles may be neglected in the approximation we use when evaluating the $M^{(w)}$ and $M^{(z)}$ which considerably simplifies the calculations. The resulting expression for $M^{(w)}$ is:

$$M^{(w)} = i \frac{G_F^2}{16\pi^2} \sin\theta \cos\theta (m'^2 - m^2) \ln \frac{M_w^2}{m'^2} \times$$

$$\times \bar{u}(k_1)\gamma_\rho(1+\gamma_5)u(p)\bar{u}(k_2)\gamma_\rho(1+\gamma_5)u(-k_3)-(k_1 \leftrightarrow k_2). (A.5)$$

The leading contribution to the $M^{(z)}$ term comes from Fig. 2d with the virtual W-boson: it contains the factor $\ln \frac{M_w^2}{m'^2} \gtrsim 20$ (remember that $M_w \gtrsim 40$ GeV, $m' < 1$ MeV) while the contributions of the rest of the diagrams do not contain it. Taking into account only the leading contribution we have:

$$M^{(z)} = -i \frac{G_F^2}{16\pi^2} \sin\theta \cos\theta (m'^2 - m^2) \ln \frac{M_w^2}{m'^2} \bar{u}(k_1)\gamma_\rho(1+\gamma_5)u(p) \times \\ \times \bar{u}(k_2)\gamma_\rho(2(1+\gamma_5) - 8\sin^2\theta_w)u(-k_3)-(k_1 \leftrightarrow k_2). (A.6)$$

It is easy to obtain the sum:

$$M^{(w)} + M^{(z)} = i \frac{G_F^2}{2\pi\sqrt{2}} \frac{m'^2 - m^2}{M_w^2} \ln \frac{M_w^2}{m'^2} \sin\theta \cos\theta \times \\ \times \bar{u}(k_1)\gamma_\rho(1+\gamma_5)u(p)\bar{u}(k_2)\gamma_\rho(1 - \frac{1+\gamma_5}{8\sin^2\theta_w})u(-k_3)-(k_1 \leftrightarrow k_2). (A.7)$$

The comparison of the right-hand sides of (A.4) and (A.7) shows that the sum $(M^{(w)} + M^{(z)})$ is at least by an order greater than the $M^{(\gamma)}$ term, so

$$M_2 \approx M^{(w)} + M^{(z)}. (A.8)$$

In conclusion we want to note that the evaluation of the $\nu' \rightarrow \nu + \gamma$ amplitude M_3 is analogous to the evaluation of the $\mu \rightarrow e + \gamma$ amplitude. The leading contribution to the M_3 amplitude comes from the diagrams shown in Fig. 3b with the virtual W-boson.

REFERENCES

1. B. Pontecorvo. J. Exp. Theor. Phys. (USSR), 33, 549 (1957); 34, 247 (1958); 53, 1717 (1967).
2. C. Gribov, B. Pontecorvo. Phys. Lett., 29B, 493 (1969).
3. J. Bahcall, S. Frautschi. Phys. Lett., 29B, 623 (1969).
4. S. M. Bilenky, B. Pontecorvo. Phys. Lett., 61B, 248 (1976).
5. H. Fritzsch, P. Minkowsky. Preprint CALT-68-525 (1975).
6. S. Eliezer, D. A. Ross. Phys. Rev., D10, 3088 (1974).
7. S. Glashow, J. I. Iliopoulos, L. Maiani. Phys. Rev., D2, 1285 (1970).
8. S. Weinberg. Phys. Rev. Lett., 19, 1264 (1967);
A. Salam. Proc. of the Eight Nobel Symposium (J. Wiley, N.Y., 1968).
9. P. W. Higgs. Phys. Lett., 12, 1321 (1964).
10. M. K. Gaillard, B. Lee. Phys. Rev., D10, 897 (1974).
11. S. Parker, H. L. Anderson, C. Rey. Phys. Rev., 133B, 768 (1964).
12. S. Korenchenko, B. Kostin, G. Mitselmaher, K. Nekrasov, V. Smirnov. J. Exp. Theor. Phys., 70., 3 (1976).

13. B.Pontecorvo, J.Exp.Theor.Phys. (USSR),
34, 247 (1958).
14. G.'t Hooft, M.Veltman. Nucl.Phys., B44,
189 (1972).

Received by Publishing Department
on October 18, 1976.